# CURVATURE RADIATION AND POLARIZED EMISSION FROM PSR 2303+30

J. A. GIL

The Astronomical Centre of Zielona Góra and Institute of Physics, Pedagogical University

**Abstract**

We present 430-MHz Arecibo single pulse polarization measurements for PSR 2303+30. Single pulses typically consist of one or two subpulses. Each subpulse is associated with circular polarization which reverses sense near the subpulse peak and with its own swing of the position angle which does not coincide with the average position-angle curve. We attempt to explain these complicated characteristics within the framework of a coherent curvature radiation model of pulsar emission.

# Introduction

Although curvature radiation of charged bunches moving relativistically along dipolar magnetic field lines is an attractive candidate for a mechanism of pulsar radio emission, a number of difficulties have been raised. Probably the most serious are theoretical problems with bunch formation. In this paper we present the complicated polarization characteristics of single pulses in PSR 2303+30. We compare these data with model calculations based on the properties of curvature radiation. We argue that from an observational point of view coherent curvature radiation is still the best mechanism for pulsar emission. From the theoretical approach, the Goldreich-Keeley instability (1971) seems to be the only promising bunching mechanism. Pronounced microstructure observed in subpulses suggests that the pulsar magnetosphere is penetrated by a large number of thin $e^+e^-$ plasma streams, each corresponding to a micropulse observed within subpulse envelope. In such thin plasma streams the Goldreich-Keeley instability can develop, resulting in plasma bunching (Asséo, Pellat, and Sol 1983). If the wavelength of an unstable plasma wave is smaller than the characteristic wavelength of curvature radiation, then the bunches will radiate as described in this paper.

# The model

We will assume that a subpulse within an individual pulse is associated with a bundle of magnetic field lines filled with a column of an unstable electron-positron plasma injected from a sparking region at the polar cap. This column is surrounded by charge separated Goldreich-Julian (1969) plasma. If the plasma column has a structure of thin micro-streams, then the Goldreich-Keeley instability (1971) can result in bunching (Asséo, Pellat, and Sol 1983). We assume that this mechanism will produce small bunches which can radiate by means of curvature radiation at the pulsar radio frequency. We also assume that the lifetime of these bunches is larger than about $\gamma^{-3}c/\rho$, where $c$ is the speed of light, $\gamma$ is the Lorentz factor, and $\rho$ is the radius of curvature of magnetic field lines.

A geometry of subpulse emission is presented in figure 1 which represents a cross section of the plasma column (with bunches moving along magnetic field lines) in a direction perpendicular to the planes of field lines. Each field line is populated by randomly distributed bunches. Each bunch can be observed only for a time interval $\gamma^3 c/\rho$, but a continuous stream of bunches along a single field line fills with radiation a pulse region of width about $1/\gamma$. Other longitudes are irradiated by neighboring field lines. A subpulse envelope is described by a spatial modulation function $S(\varphi) = \exp(-\varphi^2/2\sigma_\varphi^2)$, where $\varphi$ is the longitude, which reflects an energy density distribution within the column. The characteristic width of the column $\sigma_\varphi$ is assumed to be larger than the beam width of elementary curvature emission $1/\gamma$. Therefore many different field lines contribute to the observed subpulse emission at a given pulse longitude $\varphi$.

Emission observed at any pulse longitude $\varphi$ (to within an accuracy of $1/\gamma$) is an incoherent superposition of contributions from a large number of bunches. Emission of each bunch propagates through an unbunched $e^+e^-$ plasma until it leaves the column. In the observer's frame of reference it can be considered as a shot-noise pulse of subnanosecond duration $\gamma^{-3}c/\rho$. The resulting emission of a large number of bunches has the characteristic of curvature-generated polarized shot noise (Gil and Snakowski 1990b).

Let us calculate the characteristics of single particle (small bunch) curvature radiation propagating through a dense anisotropic $e^+e^-$ plasma in strong pulsar magnetic field. Refraction indices for the



https://doi.org/10.1017/S0002731600155611 Published online by Cambridge University Press

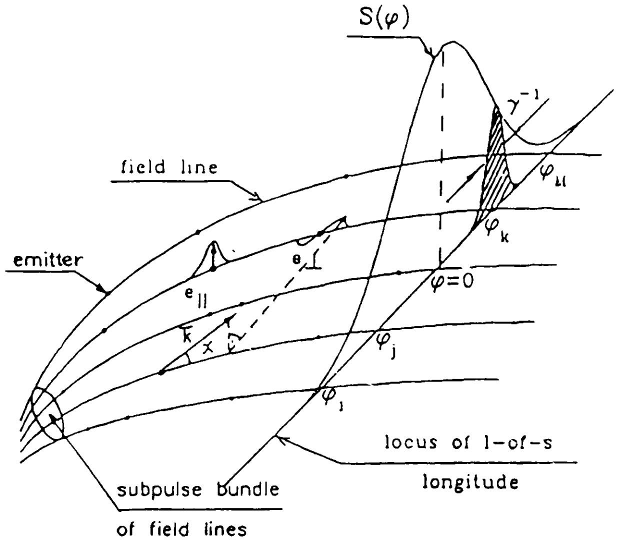


**Figure 1** Geometry of the pulsar emission region (see text for explanation).

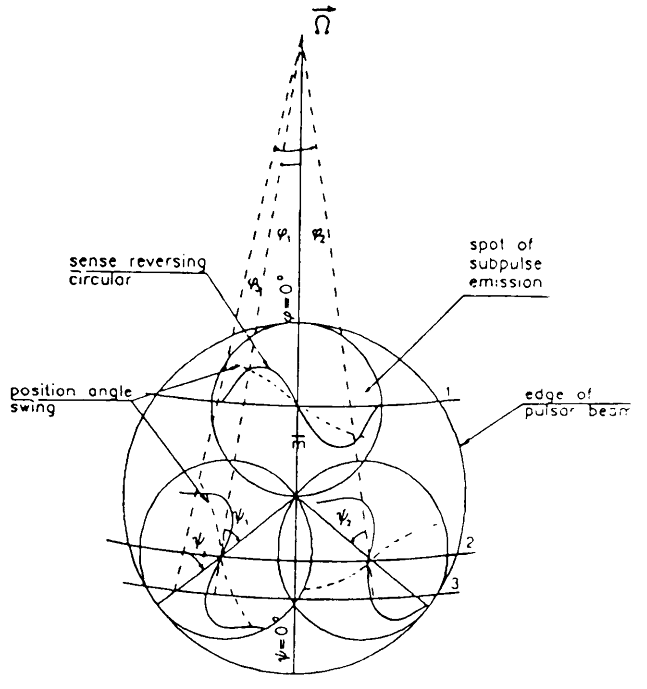


**Figure 2** Geometry of pulsar emission projected onto the celestial sphere. The beam of pulsar emission centered on the magnetic axis $\vec{m}$ is assumed to be at rest and the observer rotates around the pulsar spin axis $\vec{\Omega}$. Three spots of subpulse emission are marked. They overlap at low intensity regions. The observed longitudes are marked by Greek letters $\varphi$. Within each spot the instantenous position-angle swings across subpulses are marked by dashed lines and sense-reversing circular polarization is marked by solid lines. The Radhakrishnan and Cooke position angles are marked by Greek letters $\psi$.

propagation of electromagnetic waves within the $e^+e^-$ plasma in a strong, curved magnetic field have been obtained by Beskin *et al.* (1988). In a strong magnetic field near the pulsar, charged particles cannot move in any direction perpendicular to field lines. The radiation $E_\perp$ with polarization perpendicular to the planes of the field lines has no component in the direction of $\boldsymbol{B}$ (along which the plasma particles can move) and therefore propagates as if in a vaccum, hence $n_\perp = 1$. For the polarization $E_\parallel$ parallel to the planes of field lines, there exists a non-zero component along $\boldsymbol{B}$ in the case of propagation at the angle $\kappa$ to the local direction of $\boldsymbol{B}$ and $n_\parallel \approx 1/\cos\kappa$. Since for curvature radiation within the subpulse plasma column $\langle\kappa\rangle \leq 1/\gamma \approx 1/100$, one can estimate that $n_\parallel \approx 1.000038$. As we will see, a small difference from unity is crucial for polarization-angle behavior.

The spectrum of curvature radiation can be obtained by taking the Fourier transform of the electric field emitted by a charged particle moving along a curved trajectory in a strongly magnetized plasma (Gil and Snakowski 1990a)

$$\varepsilon_\parallel(\nu,\varphi) = \int_{-\infty}^{+\infty} \frac{\delta^2+\varphi^2-\theta^2}{\left[1-n_\parallel+(n_\parallel/2)\left(\delta^2+\varphi^2+\theta^2\right)\right]^2} \exp\left(\frac{i\nu}{2\nu_0}\right)\left[\left(\delta^2+\varphi^2\right)\theta+\frac{\theta^3}{3}\right] d\theta\,,$$

$$\varepsilon_\perp(\nu,\varphi) = \int_{-\infty}^{+\infty} \frac{2\delta\varphi}{\left[1-n_\perp+(n_\perp/2)\left(\delta^2+\varphi^2+\theta^2\right)\right]^2} \exp\left(\frac{i\nu}{2\nu_0}\right)\left[\left(\delta^2+\varphi^2\right)\theta+\frac{\theta^3}{3}\right] d\theta\,, \tag{1}$$

where $\delta = 1/\gamma$, $\varphi$ is the longitudinal angle between the plane of bunch motion and the line of sight, $\theta$ is a polar coordinate, $\nu$ is the observing frequency and $\nu_0 = \nu/2\pi\rho$ is the basic cyclotron frequency. Since in our case both $n_\parallel$ and $n_\perp$ can be regarded as unity, the resulting spectra do not differ from the vacuum case (Gil and Snakowski 1990a)

https://doi.org/10.1017/S0002731600155611 Published online by Cambridge University Press

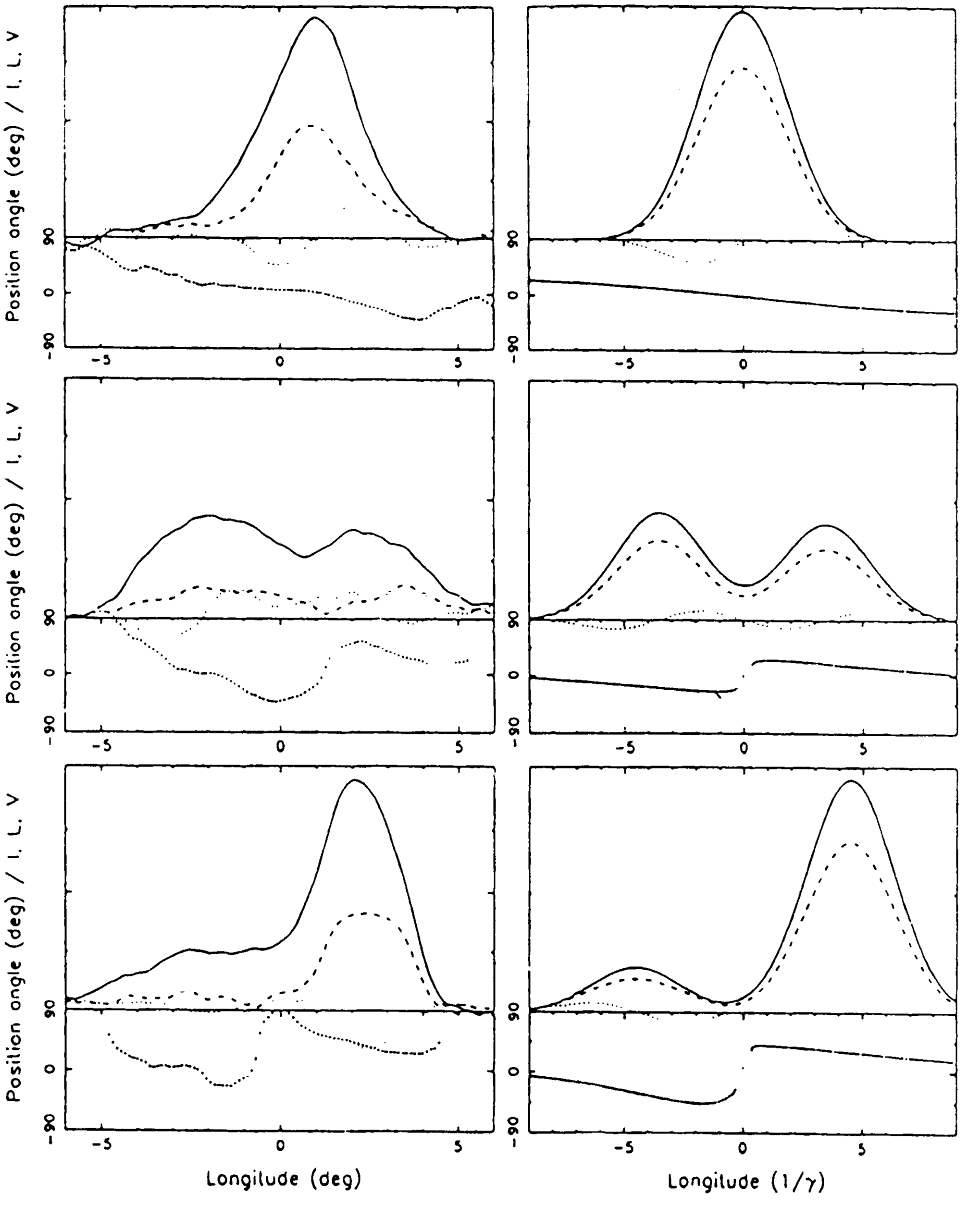


**Figure 3** The polarization characteristics of PSR 2303+30; 430 MHz data (left-hand panels); model (right-hand panels). Total intensity $I$ (solid curve), linear polarization $L$ [$= (Q^2 + U^2)^{1/2}$] (dashed curve), circular polarization (thin dotted curve) and the position angle $\psi$[$= (1/2)\arctan(U/Q)$] (thicker dotted curve). The longitude axis is scaled in degrees for the data and in $1/\gamma$ for the model, where $\gamma$ is the Lorentz factor.

$$\begin{aligned} \varepsilon_{\|}(\nu,\varphi) &= \nu\left(\delta^2+\varphi^2\right) K_{2/3}\left[\frac{\nu}{3\nu_0}\left(\delta^2+\varphi^2\right)^{2/3}\right], \\ \varepsilon_{\perp}(\nu,\varphi) &= i\nu\varphi\left(\delta^2+\varphi^2\right)^{1/2} K_{1/3}\left[\frac{\nu}{3\nu_0}\left(\delta^2+\varphi^2\right)^{2/3}\right], \end{aligned} \tag{2}$$

where $i$ is the imaginary unit, and $K_{1/3}$ and $K_{2/3}$ are modified Bessel functions. Let us note that $\varepsilon_\perp$ is purely imaginary and $\varepsilon_\|$ is real. Therefore $\varepsilon_\|$ and $\varepsilon_\perp$ are shifted in phase by exactly $\pi/2$. This means that the radiation of each small bunch is highly circularly polarized. As was shown by Gil and Snakowski (1990a) the circular polarization reverses sense at the subpulse intensity peak as observed in pulsar emission.

The electric field of the resultant emission can be written as a vector sum of contributions from a large number of bunches

https://doi.org/10.1017/S0002731600155611 Published online by Cambridge University Press

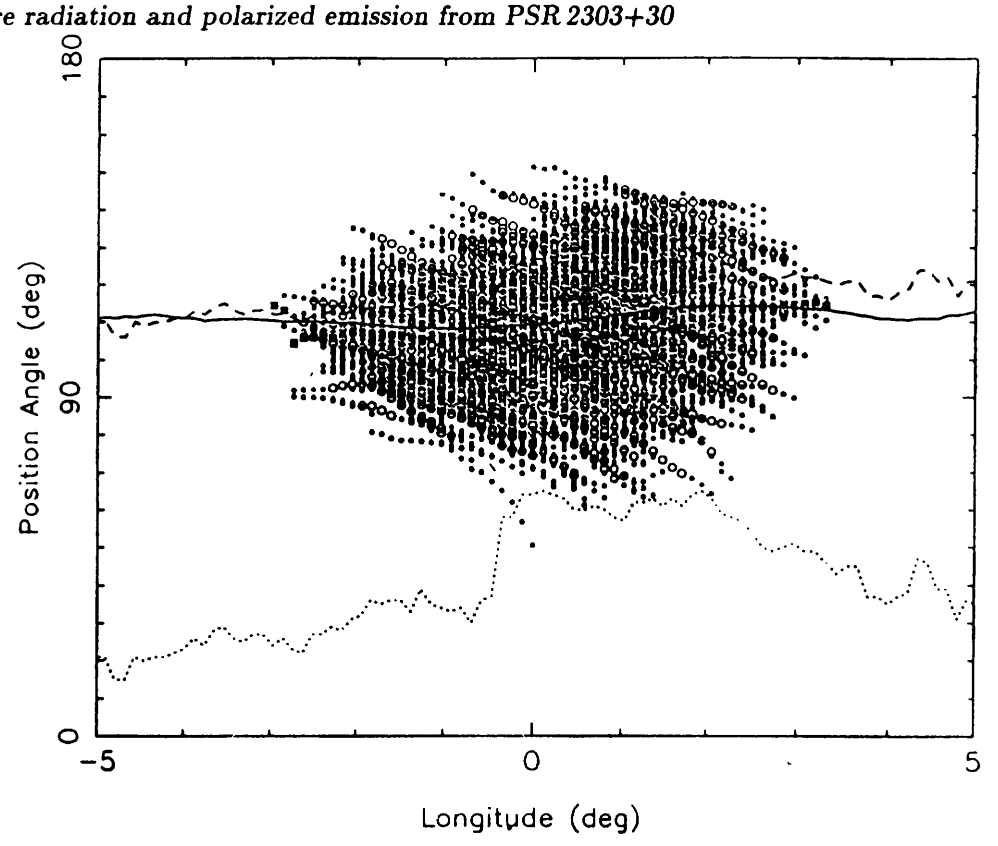


**Figure 4** Swings of the position angle across subpulses (above 50% of the peak intensity threshold) of PSR 2303+30. Open circles have size proportional to the subpulse intensity. Filled squares represent the intensity-weighted average which coincides with the total average position-angle curve.

$$E_{\parallel}(t,\varphi) = \sum_{i=1}^{N}\sum_{j=1}^{M}\sum_{k=1}^{L} e_{\parallel}(t - t_{ij}, \varphi - \varphi_j) S_k(\varphi_j)$$

and (3)

$$E_{\perp}(t,\varphi) = \sum\sum\sum e_{\perp}(t - t_{ij}, \varphi - \varphi_j S_k(\varphi_j),$$

where $t$ is the time, $\varphi$ is longitude, $t_{ij}$ is the antenna arrival time of the $i^{\text{th}}$ pulse from the $j^{\text{th}}$ field line, $N$ is the number of bunches along the field line, $M$ is the number of field lines, and $L$ is the number of spots contributing to the emission observed at the longitude $\varphi$ (figure 2). The subpulse shape is described by the Gaussian modulation function $S_k(\varphi_j)$, (figure 1). The $\parallel$ and $\perp$ indices correspond to polarization parallel and perpendicular to the planes of dipolar magnetic field lines, respectively.

The spectra can be calculated as Fourier transforms of eqs.(3)

$$\epsilon_{\parallel}(\nu,\varphi) = \sum_{i}^{N}\sum_{j}^{M}\sum_{k}^{L} \varepsilon_{\parallel}(\nu, \varphi - \varphi_j) S_k(\varphi_j) \exp(-2\pi i \nu t_{ij})$$

and (4)

$$\epsilon_{\perp}(\nu,\varphi) = \sum\sum\sum \varepsilon_{\perp}(\nu, \varphi - \varphi_j) S_k(\varphi_j) \exp(-2\pi i \nu t_{ij} - \delta_t),$$

where $\nu$ is the observing frequency, $\varepsilon_{\parallel}$ and $\varepsilon_{\perp}$ are spectra corresponding to elementary bunches, eqs.(2), and $\delta_t$ is an average time delay between parallel $e_{\parallel}$ and perpendicular $e_{\perp}$ components caused by the small anisotropy of a propagation region. This time delay can be estimated from $\delta_t = \mathcal{L}|n_{\parallel} - n_{\perp}|/c$, where $\mathcal{L}$ is the size of an intervening plasma region. If $\mathcal{L}$ is of the order of the radius of the emission region $r < 10^8$ cm, $n_{\perp} = 1$ and $n_{\parallel} = 1.000038$ then $\delta_t$ is about $10^{-7}$ s. This means that the two orthogonal

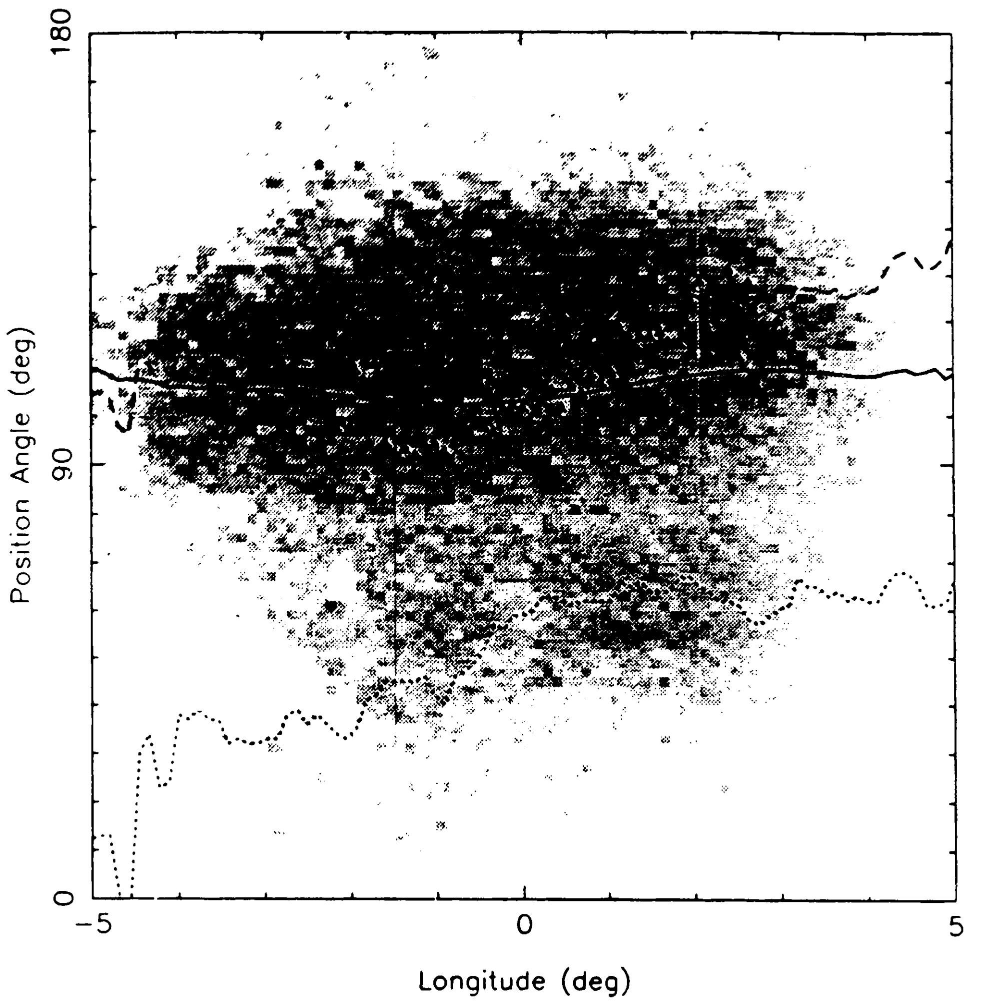


**Figure 5** Scatter plot of the PSR 2303+30 position angle *vs.* pulse longitude with quantized frequency of occurrence (grey scale) as a third axis. The black squares correspond to maximum of occurrence. Total average position-angle curve (solid) is also plotted. Triangles represent an intensity-weighted average of the position angles at the subpulse peak, which can be interpreted as a Radhakrishnan and Cooke curve. Notice the continuous position-angle swings across subpulses ranging from about 90° to 120°.

components are delayed by about $10^{-7}$ s when they leave the plasma column. This small delay causes the polarization ellipse to rotate, resulting in a swing of the position angle across the subpulse (Gil and Snakowski 1990b). These swings have nothing to do with the rotating-vector model (Radhakrishnan and Cooke 1969) except that they occur exactly around the RC value, determined by the orientation of the field line plane corresponding to the subpulse peak. We will call these swings "counter rotations", after Smith (1974) who observed them first.

The Stokes parameters $I$, $Q$, $U$, and $V$ or polarization state $I$, $L$ [$= (Q^2 + U^2)^{1/2}$], $V$, and $\Psi$[$= (1/2)\arctan(U/Q)$] can be easily computed from the spectra expressed in eqs.(4). In figure 3 we present results of calculations (right-hand panels) corresponding to frequency $\nu \approx \nu_c \approx 0.2\gamma^3 c/\rho \approx 0.4\pi\gamma^3\nu_0$ and half-maximum-half-width $\sigma_\varphi = 2.5/\gamma$.

The model calculations are compared with real data from PSR 2303+30 at 430 MHz recorded at the Arecibo Observatory in 1971 (Rankin, Campbell, and Backer 1974). Since the half-width of the observed subpulse is about 1.5°, the corresponding value of the Lorentz factor is about 100 (figure 3, right-hand panels).

We believe that the form of the pulse reflects an arrangement of sparks on the polar cap or spots of the subpulse emission on the celestial sphere (figure 2). The first pulse showing a single Gaussian-shaped subpulse corresponds to line-of-sight geometry number 1. One can see the monotonic rotation of the position angle and the reversing sense of circular polarization at the subpulse maximum (longitude $\varphi \approx 0°$). The second pulse consists of two subpulses corresponding to line-of-sight number 2 passing through two spots, $L = 2$ in eqs.(4). Each subpulse is associated with its own sense-reversing circular polarization and counter-rotation of the position angle $\psi$. The peak values of $\psi$ correspond to the

https://doi.org/10.1017/S0002731600155611 Published online by Cambridge University Press

RC model $\psi = \psi_1$ and $\psi = \psi_2$. The third pulse has similar characteristics, but it corresponds to an asymmetrical arrangement of sparks with respect to the line-of-sight trajectory. Counter rotations of the position angle in the individual pulses are also presented in figures 4 and 5. Notice a slope corresponding to the Radhakrishnan and Cooke model (triangles in figure 5).

In summary, we argue that the complicated observational characteristics of the polarized emission in single pulses of PSR 2303+30 can be easily understood within a very simple model involving coherent curvature radiation from a large number of bunches flowing along dipolar magnetic field lines. Each subpulse corresponds to a spark on the polar cap which builds a subpulse-associated plasma column in the magnetosphere. Radiation from an individual bunch is circularly polarized with sense reversal occuring in the plane of the bunch motion. An intensity gradient in the subpulse bundle preserves some a net circular polarization in the resultant emission from many bunches. The sense reversals occur at the intensity maximum (subpulse peak). Each subpulse has its own swing of position angle which has nothing to do with the Radhakrishnan and Cooke rotating-vector model except that the swing is symmetrical about the Radhakrishnan and Cooke value, reflecting an orientation of the field-line planes corresponding to the subpulse peak. Thus, the position angles at subpulse peaks reflect the geometry of pulsar emission, as described by the rotating-vector model. This is why the average position-angle curves often follow the Radhakrishnan and Cooke model even if single pulses show counter-rotations (figures 3, 4 and 5).

*Acknowledgments:* I thank Dr. J. M. Rankin for providing the observational data and helpful discussions. I also thank Dr. J. K. Snakowski for help with computing and plotting.